

Technical-economic comparison of nanofiltration and reverse osmosis in the reduction of fluoride ions from groundwater: experimental, modeling, and cost estimate

Mustapha Tahaikt^a, Soufian El-Ghizizel^{a,*}, Nodar Essafi^a, Mahmoud Hafsi^b, Mohamed Taky^a, Azzedine Elmidaoui^a

^aLaboratory of Separation Processes, Ibn Tofail University, Kenitra, Morocco, emails: Soufianelghizizel85@gmail.com (S. El-Ghizizel), tahaiktmustapha@yahoo.fr (M. Tahaikt), safi.nodar@gmail.com (N. Essafi), takymohamed@gmail.com (M. Taky), elmidaoui@uit.ac.ma (A. Elmidaoui)

^bWater Technical Assistance, Rabat, Morocco, email: hafsi.mahmoud2020@gmail.com

Received 12 July 2020; Accepted 19 November 2020

ABSTRACT

The fluoride content in many regions of Morocco exceeds acceptable standards, especially in phosphate regions like Benguerir. In this region, the hermetic effect of dental fluorosis is widespread among the population supplied directly by the wells. Fluoride contamination is attributed to phosphate deposition. In Morocco, the maximum acceptable concentration of fluorides in drinking water is 1.5 mg/L. In this context, the first aim of this work concerns the technical and economic comparison of nanofiltration and reverse osmosis in the reduction of fluoride ions. Three commercial membranes were involved in this study. This study confirms the performances of these membranes in the fluoride reduction and the compositions of the produced water obtained are similar. The Spiegler–Kedem model was applied to determine the constants of the model, namely the reflection coefficient and the coefficient of permeability for all the membranes used. In addition, the Hermia model was applied to identify the fouling mechanism of the three membranes. The parameters of the two models were optimized using the Levenberg–Marquardt algorithm which solves non-linear least-squares problems using an iterative technique. Good agreement between experimental results and model predicted results were obtained. For three membranes tested the transport mechanism is predominant by diffusion and the mechanism that describes the fouling is the cake-forming model. The technical-economic comparison of nanofiltration and reverse osmosis was performed on the basis of produced water with a fluoride content of 0.7 mg/L and the cost of the produced cubic meter by the three membranes is almost the same.

Keywords: Fluoride removal; Nanofiltration; Reverse osmosis; Spiegler–Kedem model; Fouling mechanisms; Cost estimate

1. Introduction

Water is an essential natural resource to maintain life and the environment, however, chemical composition of surface or subsurface is one of the prime factors on which the suitability of water for domestic, industrial, or agricultural purpose depends. Recent United Nations Children's

Fund (UNICEF) and World Health Organization (WHO) reports have confirmed that 748 million of people have no access to safe water of proper quality, while more than 1.8 billion of people use water contaminated with feces to potable purposes [1]. Though groundwater contributes with only 0.6% of the total water resources on earth, it is the

* Corresponding author.

major and the preferred source of drinking water in rural as well as urban areas, particularly in developing countries [1].

Due to various natural or anthropogenic ecological factors, groundwater is polluted and accessibility to water is limited. The presence of several natural and anthropogenic elements and compounds can considerably affect the quality of the water and lead to harmful health effects. According to WHO, the most dangerous inorganic substances appearing in groundwater, which reveal a global effect on human health, are fluorides and arsenic [2]. The presence of fluoride in natural water is connected with its appearance in natural minerals, local geological structure, and industrial activities [3].

Fluoride may reveal either advantageous or disadvantageous health effects, depending on their dose and exposure time [4]. While the concentration of fluorides in potable water ranging from 0.5 to 0.7 mg/L is recommended in order to avoid dental caries among children [1], their higher amount is regarded as a serious health problem. The regular consumption of water containing 1.5–4 mg/L results in bone tissue problems (fluorosis, arthritis, and osteoporosis) as well as in neurological issues, and it may lead to liver damage, carcinogenic, and gastrological effects [5].

There are more than 20 developed and developing nations that are endemic for fluorosis, namely: Argentina, U.S.A., India, Algeria, Libya, Egypt, Jordan, Turkey, Iran, Iraq, Kenya, Tanzania, South Africa, China, Australia, New Zealand, Japan, Thailand, Canada, Saudi Arabia, Persian Gulf, Sri Lanka, Syria, Morocco, etc. [6].

Due to fluoride effects on health, WHO as well as national health authorities have established its maximum permissible concentration in potable water at the level of 1.5 mg/L, while the recommended range is from 0.5 to 1.0 mg F/L [7,8]. Such concentration of fluoride in water minimizes its harmful effects on human's health.

In many regions of Morocco, the fluoride content exceeds acceptable standards. In the plateau of Benguerir (center of Morocco), where the work is conducted, the harmful effect of dental fluorosis is widespread among the population supplied directly from wells. The water in this region usually exceeds the fluoride standards and is often brackish. The fluoride contamination in this region is attributed to the phosphate deposit [8].

Until today, the National Office of Water and electricity (ONEE) in Morocco has resorted to dilution to avoid the frequent seasonal fluoride excesses. The decrease in water resources, especially groundwater, and the frequent fluoride excesses observed during these last decades, makes this solution unattainable. So to prevent this situation, ONEE has initiated studies to investigate remedial options.

Due to the high solubility of fluorides in water, its defluorination is difficult and expensive process [1]. Different water defluorination methods have been investigated: precipitation [9,10], ion exchange [11,12], adsorption [13,14], and membrane processes [7,8,15].

To remove fluoride and salinity from brackish groundwater in a village in Senegal, Diawara et al. [16] used low pressure OI and obtained 97%–98.9% fluoride retention. Gedam et al. [17] found a fluoride removal rate of 95%–98% from groundwater in Chandrapur village in Moradgaon region using a polyamide RO membrane. Schoeman [18]

has applied RO for defluorination of water in parts of South Africa with initial concentrations of fluoride ranging from 10 to 17 mg/L and the concentration in the obtained permeate was 0.2 mg/L. Briao et al. [19] used OI for desalination of groundwater from the Guarani region in southern Brazil, 100% fluoride retention was obtained.

Elazhar et al. [20] used the spiral-type membranes NF90 (Filmtec, USA) and the fluoride ion retention rate obtained was 97.8%. With a membrane of the type (DK-5) of the spiral type, Bannoud and Darwich [21] obtained a retention rate of 60%. Pontié et al. [22] used a polyamide membrane NF45 (Filmtec, USA), the initial fluoride ion concentration is 0.02 M. The retention rate was 91% for a NaF solution. Tahaikt et al. [7] compared the effectiveness of removing fluorides from water using three commercial polyamide membranes: NF90 (Filmtec, USA), NF270 (Filmtec, USA), and TR60 (Toray, Japan) for different fluoride content, and they obtained rejection rates which vary with the initial fluoride content but exceed 74% for the NF270 and TR60 membranes, and on the other hand, for NF90 membrane the rejection rate exceeds 98% and is less sensitive to the initial fluoride concentration.

In comparison with reverse osmosis, nanofiltration membranes have a low retention of monovalent ions, but a significant rejection of bivalent and multivalent ions and organic substances [23]. The permeate obtained by reverse osmosis must be remineralized. Depending on the cut-off threshold of the nanofiltration membranes, the physico-chemical quality of the permeate may be satisfactory.

To study the transfer mechanism through reverse osmosis membranes and nanofiltration, Zouhri et al. [24] applied the Speigler–Kedem model on five membranes: two reverse osmosis membranes (TM710 (Toray, Japan), and BW 30LE (Filmtec, USA)) and three nanofiltration membranes (NF90 (Filmtec, USA), NF270 (Filmtec, USA), and TR60 (Toray, Japan)), during the desalination of the waters of M'irt (Morocco). They found that both transfer modes (convection and diffusion) occur for NF270 and TR60 membranes. For the NF90 and RO membranes, the transport of solutes is essentially diffusional.

In order to reduce the concentration of fluoride and improve the quality of drinking water for the population, and since the year 2000, ONEE and Ibn Tofail University have collaborated to study and compare the performances of electro dialysis, nanofiltration, and reverse osmosis in the reduction of fluoride ions in Benguerir groundwaters.

In previous papers, studies were carried out on fluoride removal from underground water by electro dialysis pilot plant with a capacity of 1 m³/h and by a nanofiltration pilot plant having a high pressure pump with a maximal pressure of 70 bar. Many articles from this collaboration have been published [7,8,15].

The aim of this work concerns the technical and economic comparison of nanofiltration and reverse osmosis in the reduction of fluoride ions. The Speigler–Kedem model, described by Zouhri et al. [24], was applied to determine the constants of the model, namely the reflection coefficient and the coefficient of permeability for all the membranes used. In addition, the Hermia models modified by Field et al., described by Charfi et al. [28] was applied to identify the fouling mechanism of the three membranes.

The technical-economic comparison of nanofiltration and reverse osmosis was performed on the basis of produced water with a fluoride content of 0.7 mg/L. The details of the calculation are illustrated by Elazhar et al. [20] and Lahnid et al. [31].

2. Experimental

The experiments were performed on an NF/RO pilot plant (E 3039) supplied by TIA Company (Technologies Industrielles Appliquées, France) shown in Fig. 1. The applied pressure over the membrane can be varied from 5 to 70 bar with manual valves.

The pilot plant is equipped with two identical pressure vessel operating in series. Each pressure vessel contains one element. The pressure loss is about 2 bars corresponding to 1 bar of each pressure vessel. The two spiral wound modules are equipped with two commercial membranes of one type. Table 1 gives the characteristics of the membranes used. After the run, the membranes were cleaned with alkaline and acidic cleaning solutions according to the manufacturer’s recommendations.

The temperature was kept at 29°C using the heat exchanger. Samples of permeate were collected and water parameters were determined analytically following standard

methods previously described [7,8,15]. Some other parameters were followed such as flux of the permeate given by the equation:

$$J_v = \frac{Q_p}{S} \left(\frac{L}{m^2 \cdot h} \text{ or } \frac{m^3}{m^2 \cdot s} \right) \tag{1}$$

where S is membrane surface area (m^2), Q_p is the flow rate of the permeate L/h or m^3/s .

The second parameter is the recovery rate Y (%) which is defined as:

$$Y(\%) = \frac{Q_p}{Q_0} \times 100 \tag{2}$$

where Q_p is the permeate flow (L/h), Q_0 is the feed flow (L/h).

The third parameter is the salt rejection R which is defined by Eq. (3) above.

$$R = \left(1 - \frac{C_p}{C_0} \right) \tag{3}$$

where C_p is the solute concentration in permeate (g/L), C_0 is the solute concentration in feed water (g/L).

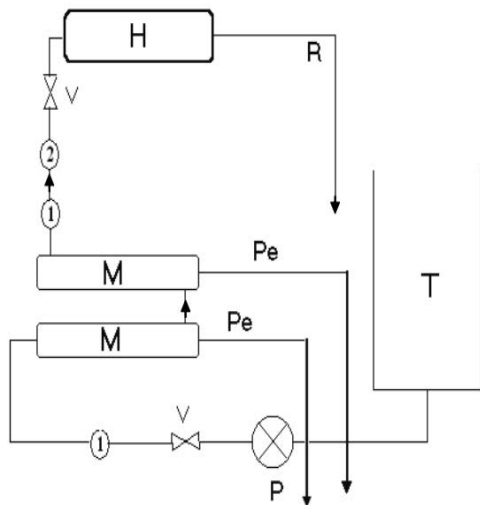


Fig. 1. Schematic diagram and picture of the nanofiltration/reverse osmosis pilot plant. T: tank; P: feed pump; V: pressure regulation valves; M: nanofiltration module; Pe: permeate recirculation; R: retentate recirculation; H: heat exchanger; 1: pressure sensor; 2: temperature sensor.

Table 1
Characteristics of the membranes used

Membrane	MWCO (Da)	Area (m^2)	Salt rejection (%)	P_{max} (bar)	pH	Material
NF90 4040	90	7.6	97% (1)	41	3–10	Polyamide
BW 30LE4040	–	7.2	99.5% (2)	41	2–11	Polyamide
TM710	–	8.1	99.7% (3)	41	2–11	Polyamide

- Salt rejection based on the following test conditions 2,000 ppm $MgSO_4$, 77°F (25°C), and 15% recovery rate at the pressure 4.8 bar.
- Salt rejection based on the following test conditions 2,000 ppm NaCl, 77°F (25°C), and 15% recovery rate at the pressure 10 bar.
- Salt rejection based on the following test conditions 2,000 ppm NaCl, 77°F (25°C), and 15% recovery rate at the pressure 15.5 bar.

The experiments were conducted on underground water of Benguerir plant. The analytical results of the feed water are shown in Table 2.

3. Results and discussions

3.1. Effect of pressure and Spiegler–Kedem model fitting

3.1.1. Effect of pressure

The study of the pressure effect on the physico-chemical quality of the permeate has carried out in batch mode. Fig. 2 shows the variation of the permeate flux, conductivity, fluoride content, pH, Langelier index, hardness, and alkalinity as a function of the pressure.

Analysis of these results shows that the permeate flux (Fig. 2a) increases almost linearly with the pressure applied according to Darcy's law for the three membranes studied. The increase in pressure improves the driving forces and overcomes the resistance of the membranes. Better flow was obtained by the NF90 membrane. The permeate flux follows the following order: NF90 > BW30LE4040 > TM710.

For the three membranes, the physico-chemical parameters are close and below the limit value for drinking water.

For pressures below 30 bar, the conductivity of the permeate (Fig. 2b) decreases with the increase in pressure for the TM710 and BW 30LE membranes, then beyond that, a plateau is formed. For these two membranes, the rate of demineralization reaches 98.7%. On the other hand, for the NF90 membrane, the conductivity decreases with the increase in pressure, but beyond 25 bar the conductivity of the permeate begins to increase and the demineralization rate achieved is 98%.

BW30LE4040, TM710, and NF90 membranes significantly reduce fluoride ions (Fig. 2c), and this decrease is more pronounced with increased pressure and achieves removal rates of 100% for TM710 and BW 30LE membranes and 98.76% for NF90 membrane.

A slight variation in pH and Langelier index (Figs. 2d and e) in the permeate is observed. The values of the Langelier index show a high aggressiveness of the obtained water. The pH values obtained for the NF90 membrane are higher

than those obtained for the other two membranes. This is due to the concentration of CO_2 which crosses these membranes and also to the salinity and alkalinity of the permeate according to the following relationships:

$$\text{pH} = pK_1 - \varepsilon + \log[\text{HCO}_3^-] - \log[\text{CO}_2] \quad (4)$$

$$\text{pH}_s = pK_2 - pK_s + 2\varepsilon - \log[\text{Ca}^{2+}] - \log[\text{HCO}_3^-] \quad (5)$$

with ε is expressed as a function of the ionic strength μ of the

$$\text{solution } \varepsilon = \frac{\sqrt{\mu}}{1 + \sqrt{\mu}}.$$

where pK_1 , pK_2 , and pK_s are the acidity constants of carbonic acid and hydrogen carbonate, and the solubility product of calcium carbonate [33]. The more salinity and alkalinity increases, the more the pH of the solution increases.

Alkalinity and hardness (Figs. 2f and g) of the permeate obtained by the three membranes are very low and a slight decrease with increasing pressure was observed. Almost 100% hardness rejection were achieved for all three membranes. For alkalinity, rejection of 93.75% and 99% were obtained for the NF90 membrane and for the two membranes TM710 and BW 30LE, respectively.

These results obtained by NF90 can be explained by the structure of this membrane, which is close to RO membranes ones and the predominant mode of salt transport across these membranes is achieved by diffusion [7,24]. In general, the effect of pressure is controlled by two different phenomena with opposite effects in the separation of the ions; firstly, the increase in pressure causes an increase in the solvent flux, but the ion fluxes remain unchanged due to the retention of ions by the steric/charge interactions and secondly, the concentration polarization phenomenon decreases the effect of charge and thus produces an increase in the solute transfer through the membrane and consequently decreases the rejection [26].

3.1.2. Spiegler–Kedem model fitting

To understand the performance of the NF90 membrane in comparison with those of the BW30LE and TM710 membranes in the reduction of fluoride ions, the model of Spiegler–Kedem was applied to describe the transport of solutes in the membranes studied especially fluoride ion.

The Spiegler–Kedem model is based on irreversible thermodynamics considers the membrane as a "black box." By introducing the local transport coefficients, Spiegler–Kedem obtained the following equations:

$$J_v = -L_p \left(\frac{dp}{dx} - \sigma \frac{d\pi}{dx} \right) \quad (6)$$

$$J_s = -\bar{P} \frac{dC_s}{dx} + (1 - \sigma) C_s J_v \quad (7)$$

where L_p , p , x , π , \bar{P} , C_s , and σ represent, respectively, the hydraulic permeability, the pressure, the distance, the osmotic pressure, the local permeability of the solute, the

Table 2
Characteristics of the feed water

Parameter	Feed water	Moroccan guidelines [34]	WHO [35]
Temperature, °C	29	–	–
Turbidity, NTU	<2	–	–
pH	7.41	6–9.2	6.5–8.5
pHs	7.80	–	–
Conductivity, $\mu\text{s}/\text{cm}$	1,492	2,700	–
Hardness, mg/L CaCO_3	440	500	500
Alkalinity, mg/L CaCO_3	320	200	–
Fluoride, mg/L	2.32	1.5	1.5
Sulfate, mg/L	116	200	200
Nitrate, mg/L	20	50	50
Chloride, mg/L	560	750	250

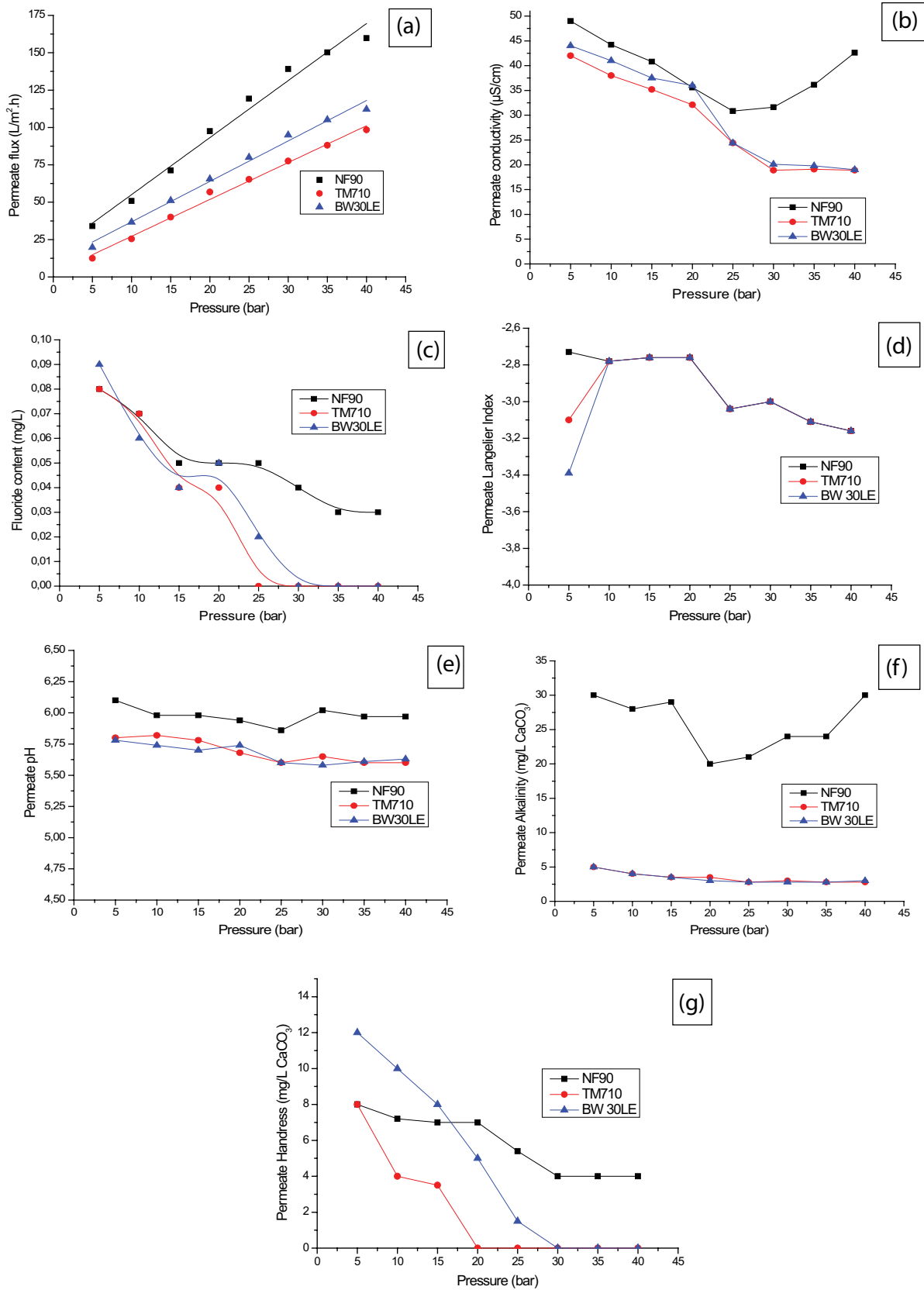


Fig. 2. Variation of (a) permeate flux, (b) conductivity, (c) fluoride content, (d) Langelier index, (e) pH, (f) alkalinity, and (g) hardness as a function of pressure.

solute concentration in the membrane, and the reflection coefficient. According to Eq. (7), the solute flux is the sum of diffusive and convective terms. Transport of the solute by convection is due to an applied pressure gradient across the membrane. The concentration difference on the membrane side and the permeate results in transport by diffusion.

The integration of these equations combined with the relation of the rejection rate and by considering the limiting conditions of the problem (for $x = 0$, $C_m = C_p$ and for $x = \Delta x$, $C_m = C_p$) lead to the following relations:

$$J_v = L_p (\Delta P - \sigma \Delta \pi) \quad (8)$$

$$R = 1 - \frac{C_p}{C_f} = \frac{\sigma(1-F)}{1-\sigma F} \quad (9)$$

$$\text{with } F = \exp\left(\frac{(1-\sigma)J_v}{P_s}\right)$$

where ΔP is the transmembrane pressure. $\Delta \pi$ is the difference in osmotic pressure on either side of the membrane (bar). C_f , C_p , and C_m is the concentrations, respectively, in feed, permeate, and in the membrane. L_p is the hydraulic permeability of the membrane. σ is the reflection coefficient. P_s is the solute permeability. Δx is the membrane thickness [24].

The following assumptions were made while using the Spiegler–Kedem model in this research:

- The driving forces are pressure and concentration gradients.
- The model predicts the transport of the solute and solvent through the membrane irrespective of the type of solute, charge, solvent, and membrane [25].

Fig. 3 shows the variation of permeate flux as a function of the pressure and the fitting using Spiegler–Kedem model. A summary of the transport parameters (σ , P) determined for the membranes studied is presented in Table 3.

The result shows a good fit of the permeate flux as a function of pressure and for the retention rate of all ions as a function of the permeate flux values for all membranes used.

The reflection coefficient σ and the permeability to the solvent P obtained for the three membranes are close. The permeability follows the following order: NF90 > BW30LE4040 > TM710.

Fig. 4 shows the experimental data of rejection rates of HCO_3^- , F^- , NO_3^- , Cl^- , SO_4^{2-} , Mg^{2+} , and Ca^{2+} as a function of the permeate flux for the three membranes and the

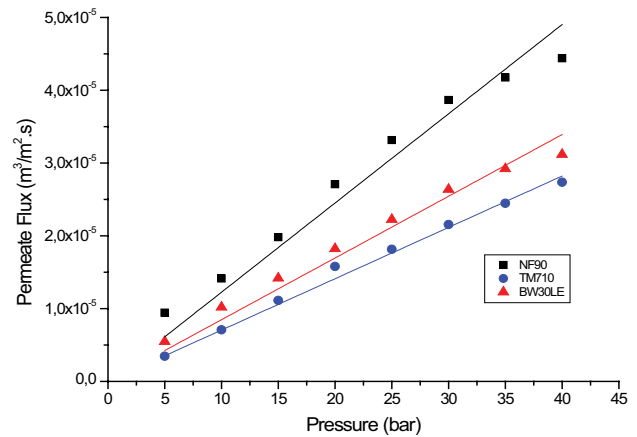


Fig. 3. Variation of the permeate flux as a function of the pressure and the fitting using Spiegler–Kedem model.

fitting using Spiegler–Kedem model. Table 4 shows the transport parameters (σ , P) obtained during the process.

The results show that the three membranes exhibit a complete retention for all ions. According to Spiegler–Kedem model these membranes have a high reflection coefficients σ which nearly equal to the unity for all ions studied. High reflection coefficient indicates convection transport is almost totally sterically hindered [26] and the predominance of the diffusion contribution especially for reverse osmosis membranes. For NF membranes the separation mechanism is highly complex, in addition to the diffusion, the mechanism includes the effect of dielectric exclusion which is caused by the interactions of ions with the bound electric charges induced by ions at the interfaces between media of different dielectric constants, in particular, membrane matrix and solvent [27].

In NF membranes, the high rejection of fluoride anion is attributed mainly to steric and charge effects and although to its very small size and more strongly hydrated shell, to its high strongly charge density [27], to high pH which changes the charge of the membrane surface and makes the surface negative from the deprotonation of carboxyl functional groups ($\text{COOH} \rightarrow \text{COO}^-$) [27], to the classical Donnan equilibrium due to the existence of co-ions and to the membrane charge neutralizing effect due to cation concentration [26].

3.2. Effect of recovery rate and fouling identification

3.2.1. Effect of recovery rate

To study the effect of the recovery rate and to identify the membranes fouling mode, tests were carried out in

Table 3
Transport parameters (σ , P) determined by Spiegler–Kedem model

	NF90	TM710	BW30LE
Permeability to solvent P ($\text{m}^3/\text{m}^2 \text{ s}$)	1.225×10^{-6}	7.0537×10^{-7}	8.478×10^{-7}
Reflection coefficient σ	1.130×10^{-14}	4.6401×10^{-13}	1.131×10^{-14}
Adj. R-square	0.94	0.98	0.96

Table 4
Transport parameters (σ , P_s) determined by Spiegler–Kedem model for the studied ions

		NF90	TM710	BW30LE
F ⁻	Permeability to solute P_s (m ³ /m ² s)	4.450×10^{-8}	2.852×10^{-9}	4.326×10^{-9}
	Reflection coefficient σ	0.980	0.996	0.996
	Adj. R-square	0.988	0.998	0.999
Cl ⁻	Permeability to solute P_s (m ³ /m ² s)	3.805×10^{-8}	1.484×10^{-8}	2.520×10^{-8}
	Reflection coefficient σ	0.997	0.979	0.977
	Adj. R-square	0.999	0.999	0.999
HCO ₃ ⁻	Permeability to solute P_s (m ³ /m ² s)	1.883×10^{-7}	7.488×10^{-9}	9.681×10^{-9}
	Reflection coefficient σ	0.925	0.990	0.990
	Adj. R-square	0.999	0.999	0.999
NO ₃ ⁻	Permeability to solute P_s (m ³ /m ² s)	4.258×10^{-7}	1.215×10^{-7}	1.527×10^{-7}
	Reflection coefficient σ	0.865	0.917	0.925
	Adj. R-square	0.987	0.988	0.996
SO ₄ ²⁻	Permeability to solute P_s (m ³ /m ² s)	2.641×10^{-19}	7.890×10^{-19}	5.54×10^{-21}
	Reflection coefficient σ	1	1	1
	Adj. R-square	1	1	1
Ca ²⁺	Permeability to solute P_s (m ³ /m ² s)	3.505×10^{-8}	7.985×10^{-10}	1.062×10^{-9}
	Reflection coefficient σ	0.981	0.999	0.985
	Adj. R-square	0.999	0.999	0.999
Mg ²⁺	Permeability to solute P_s (m ³ /m ² s)	3.233×10^{-9}	2.087×10^{-8}	1.171×10^{-8}
	Reflection coefficient σ	0.997	0.997	0.989
	Adj. R-square	0.999	0.998	0.998

semi-batch mode with a pressure of 10 bar and to prevent the phenomenon of precipitation in the brine, a dose of 2 mg/L of antiscaling (Hypersperse AF200, Betz Dearborn Co., USA) has been added in the feed tank.

Fig. 5 shows the variation of permeate flux and its physicochemical parameters as a function of recovery rate for the three membranes studied. It appears that NF90, TM710, and BW30LE membranes exhibit a roughly similar behavior.

The decrease in the permeate flux (Fig. 5a) with the increase in the recovery rate is due to the semi-batch configuration adopted in this work. Indeed, in this configuration, the concentrate flow returns to the feed tank causing a significant increase in ion concentration and salinity, which in turn leads to an increase in osmotic pressure.

Figs. 5b–g shows a slight increase in all the other physico-chemical parameters in the permeate but they remain largely lower than the Moroccan standards and those recommended by the WHO. This comportment is due to the recycling of the concentrate from the membranes in the feed tank. The precipitation in the concentrate occurred at conversion rate of 84% for NF90 and 80% for both TM710 and BW30LE. The fluoride concentration in the permeate for all membranes and for the recovery rates reached (84% for NF90, 80% for TM710, and BW30LE) doesn't exceed 0.5 ppm (0.5 ppm for NF90, 0.3 for TM710, and BW30LE).

3.2.2. Fouling identification: Hermia model

In order to determine the fouling mode responsible of water flux decline the study was performed on the three membranes in semi-batch powered mode. Then,

we consider the expressions of the flux relating to the four fouling mechanisms of Hermia model modified by Field et al. [28] who inserted a deposit erosion parameter in the case of tangential filtration. More precisely, we consider the permeate flow as a function of time, we set the value of the initial flow J_0 and we optimize the parameters K_{cf} , K_{pc} , K_{ib} , and K_{cb} which correspond to each fouling mechanisms (cake formation, pore constriction, intermediate blockage, and complete blockage). These parameters have been optimized using the least squares method and their expressions obtained by analytical resolution of the model are respectively:

$$K_{cf} = \frac{\alpha C \mu p}{\rho_s \Delta P}, K_{ib} = \frac{C}{\rho_s h}, K_{pc} = \frac{2C J_0^{\frac{1}{2}}}{\rho_s e}, K_{cb} = \frac{J_0}{\rho_s h}. \quad (10)$$

All those parameters are described in Charfi et al. [28].

Fig. 6 shows the curves of the experimental and modeling data using the Hermia model for the three membranes. The parameters K_{cf} , K_{pc} , K_{ib} , and K_{cb} obtained from the modeling of the fouling for these membranes are presented in the Table 5.

The curves have two parts, the first is characterized by a significant drop in the flow of permeate as a function of time and the second by the stabilization of the flow of permeate. Usually, membrane fouling occurs during increase in TMP to maintain a particular flux or during a decrease in flux when the system is operating at constant pressure [30].

The analysis of the values of the optimized parameter K_{cf} (cake formation) reveals values greater than those reported

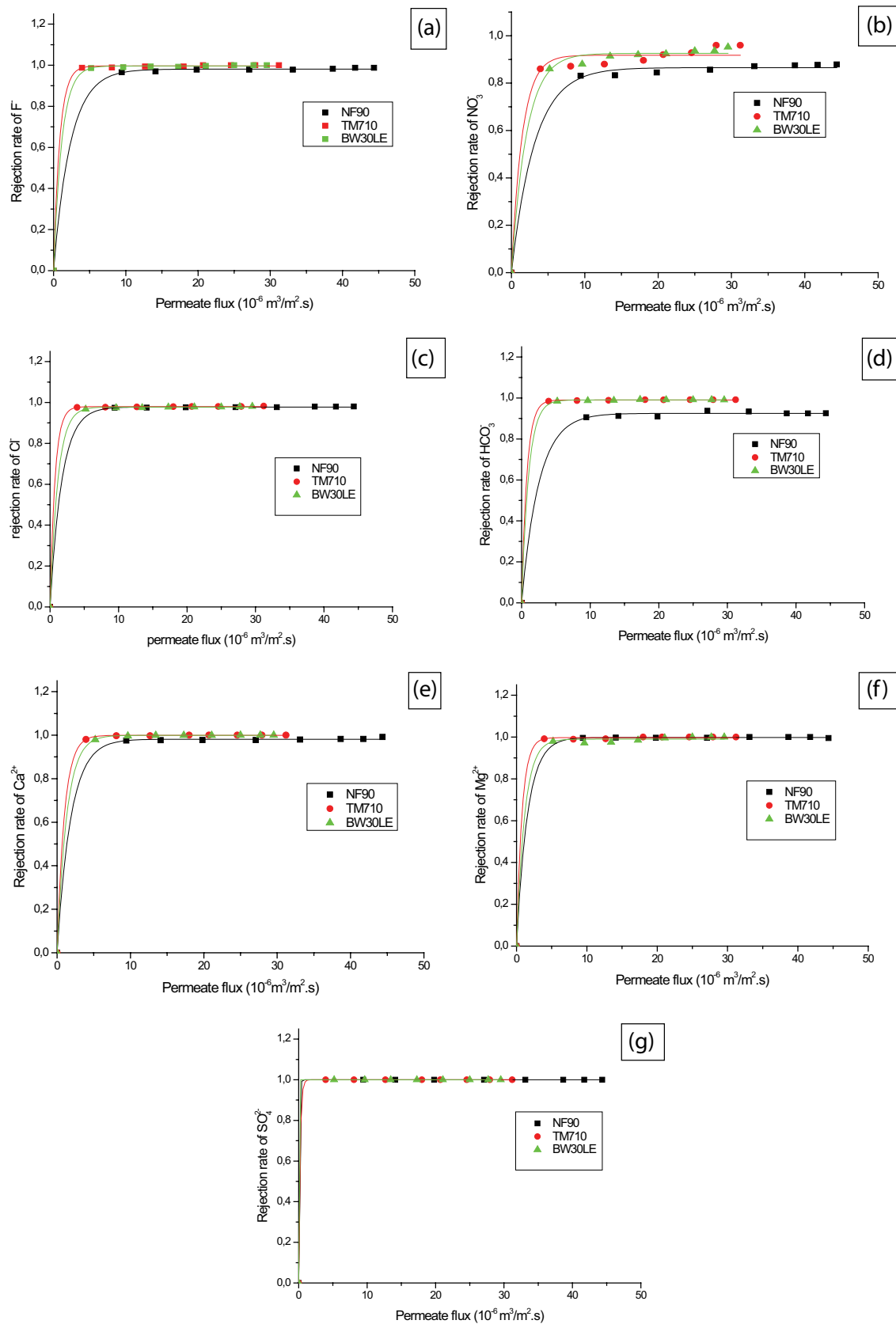


Fig. 4. Experimental data of rejection of (a) F^- , (b) NO_3^- , (c) Cl^- , (d) HCO_3^- , (e) Ca^{2+} , (f) Mg^{2+} , and (g) SO_4^{2-} , as a function of permeate flux for the three membranes and fitting using Spiegler–Kedem model.

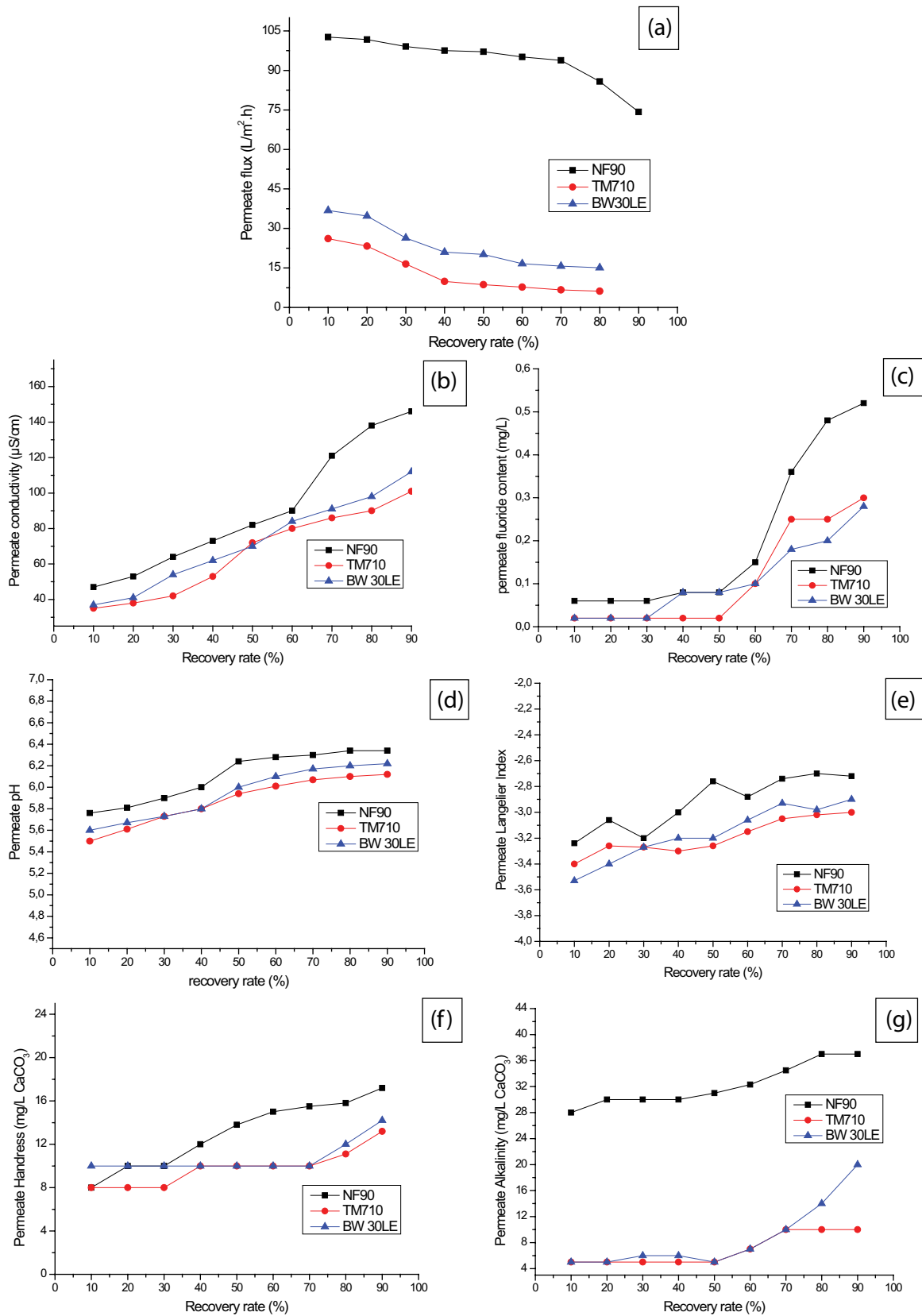


Fig. 5. Variation of permeate flux and its physicochemical parameters (a) permeate flux, (b) permeate conductivity, (c) permeate fluoride content, (d) permeate pH, (e) permeate Langelier index, (f) permeate hardness, and (g) permeate alkalinity as a function of recovery rate for the three membranes studied.

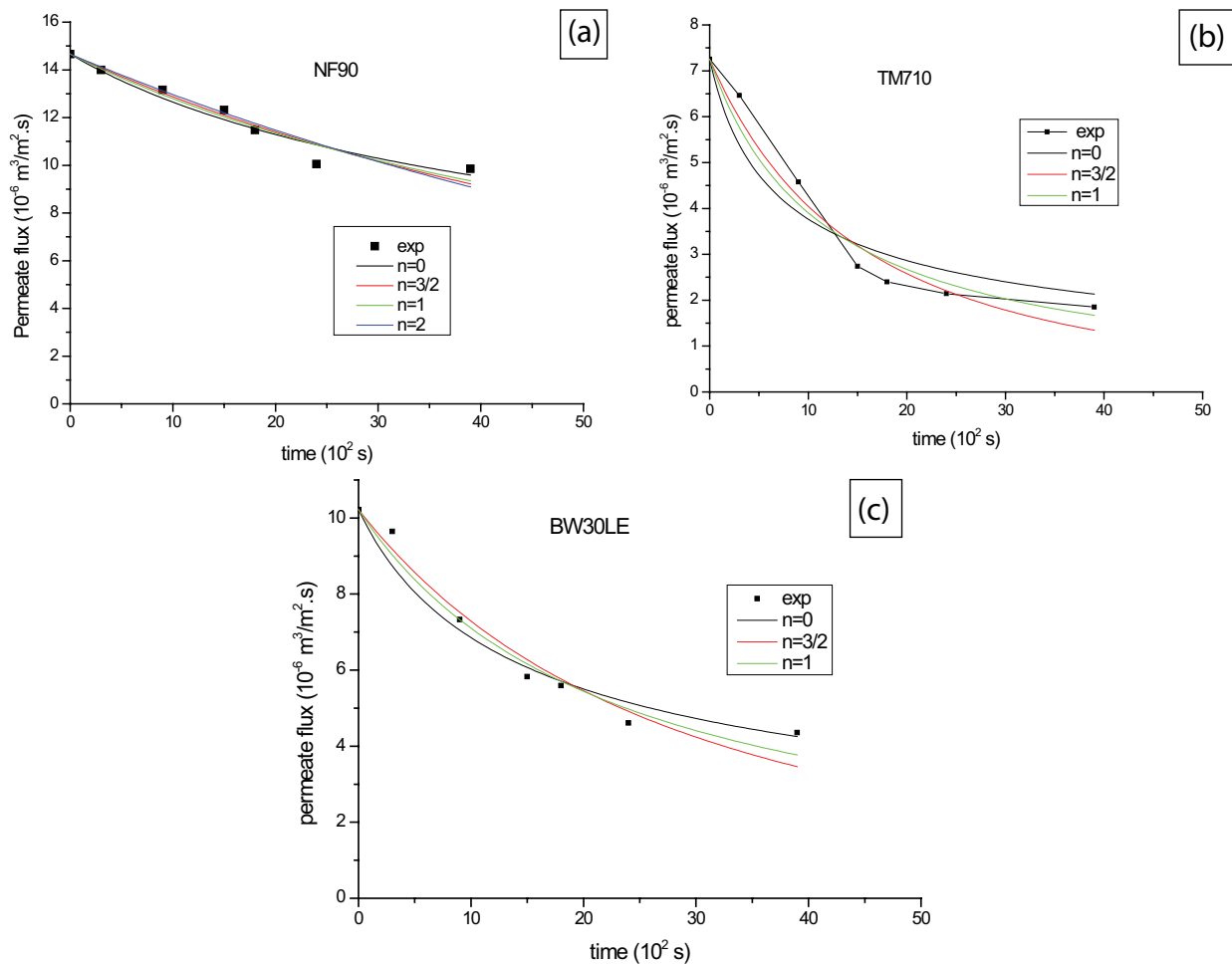


Fig. 6. Experimental and modeling data using the Hermia model for the three membranes: (a) NF90, (b) TM710, and (c) BW 30LE.

Table 5
Fouling modeling constants for the three membranes

	NF90		TM710		BW30LE	
	K_i	R -square	K_i	R -square	K_i	R -square
K_{cf} (s m^{-2})	7.97×10^5	0.96	2.57×10^7	0.91	5.859×10^6	0.96
K_{pc} ($\text{s}^{-1/2}$)	0.034	0.94	0.25	0.96	0.11	0.96
K_{ib} (m^{-1})	9.23	0.94	51.23	0.96	42.98	0.97
K_{cb} (s^{-1})	1.22×10^{-4}	0.93	-	-	-	-

in literature for the ultrafiltration membranes, which are the seat of a cake-fouling mode. This value is of the order 10^5 and largest the constant K_{cf} , the more predominant the cake-fouling mode [28].

The others optimized parameters K_{pc} and K_{ib} , indicators respectively of pore constriction and intermediate blockage fouling modes are much considerably lower than those reported in the literature for UF membranes [28]. In the case of complete blocking fouling mode, the model does not converge except for NF90 and the value obtained is much lower than those of the literature for UF, which shows that

the contribution of these types of fouling is negligible in our case. These results are explained by the dense structure of these membranes, which promotes surface fouling.

It appears that the mechanism that describes the experimental data for the three membranes tested is the cake-forming model and that can be explained by the accumulation of the retained molecules on the membrane surface (polarization of concentration and formation of the gel). This accumulation causes an increase in the hydraulic resistance of the system, which leads to a decrease in the permeate flow

4. Economical evaluation of the fluoride removal

The economic evaluation of the cost of the produced cubic meter requires the calculation of the investment and the operating cost. These parameters are determined from the membrane surface, the permeate flux, the recovery rate, and the outlet concentrations.

Economic evaluation is carried out for a plant of fluoride removal having a capacity of 2,400 m³/d (100 m³/h) corresponding to a water consumption of 50,000 capita following the Moroccan standards in rural areas. The design of this plant was performed according to the predetermined optimized conditions corresponding to a recovery rate of 80%, a fluoride content in the produced water of 0.7 ppm and a pressure pump of 10 bar for all membranes studied.

For the evaluation cost, we have adopted the model already described in the previous paper which estimates the cost of m³ of water treated by nanofiltration with remineralization by lime saturator and by electrodialysis [20,31].

A simple pre-treatment system is carried out by sand filter of 5 µm, with capacity of 125 m³/h filled with sand. The calculation of the NF/RO group is carried out on the basis of the flow rate obtained experimentally. The economical evaluation of the cost of the produced cubic meter requires the calculation of the capital cost, the operating cost, membrane replacement costs, and the energy cost. The capital cost includes the cost of system itself and its foundation on its place. In our case, the total capital cost includes: construction and building, cost of pre-treatment step, cost of NF and RO group, cost of auxiliary equipment, and cost of various services. Annual operating cost covers all expenditure incurred after plant commissioning and during actual operation, these include: amortization or fixed charges and membrane replacement. The energy cost is based on the average price of energy in Morocco which is 0.085 €/kWh.

The post-treatment consists of mixing the raw water with permeate to have a fluoride concentration of 0.7 ppm.

This method was chosen because it appears less expensive [32]. Table 6 gives the flow rates of permeate and raw water and the physico-chemical qualities of the mixtures obtained for different membranes.

Table 7 shows the cost of the produced cubic meter and the calculate capital cost, the operating cost, membrane replacement costs, and the energy cost.

The results show that the cost of the produced cubic meter is almost the same for the three membranes however defluoridation with NF membrane slightly less expensive in comparison with the other two membranes. The cost follows the following order: NF90 < BW30LE4040 < TM710.

In the literature, Elazhar et al. [20] have estimated the cost of defluoridation of brackish water by nanofiltration followed by remineralization by lime saturator as post-treatment. The total cost has been estimated at 0.212 €/m³. For the same water and the same design conditions, Lahnid et al. [31] estimated the total cost of defluoridation by electrodialysis and they obtained 0.154 €/m³ [31]. For an existing NF desalination plant in Florida with a capacity of 53,000 m³/d of groundwater, Bergman gave a total treatment cost of 0.23 €/m³ [29]. For several plant capacities, Wiesner et al. [29] have estimated to 0.24, 0.32 €/m³ the cost of the treatment of surface water for drinking water production by NF. For an RO desalination plant with a capacity less than 20 m³/d, Tzen indicated a total treatment cost is between 3.81 and 8.75 €/m³ [29]. For capacities of 20 and 1,200 m³/d, Karagiannis and Soldatos estimated the cost of treatment at 0.20 and 0.27 €/m³. For capacities of 40,000 and 46,000 m³/d, Afonso et al. and Avlonitis [29] indicated a cost of 0.22 and 0.46 €/m³.

5. Conclusion

In this work, RO and NF have been investigated on drinking water of Benguerir plant (Morocco) using two RO membranes (TM710 et BW30LE) and one NF membrane

Table 6
Permeate and raw water flow and the physico-chemical qualities of the mixtures obtained for different membranes

	Permeate flow (L/h)	Raw water flow (L/h)	Conductivity (µS/cm)	F ⁻ (mg/L)	Alkalinity (mg/L CaCO ₃)	Hardness (mg/L CaCO ₃)	NO ₃ ⁻ (mg/L)	Cl ⁻ (mg/L)	SO ₄ ²⁻ (mg/L)
NF90	81,133	18,867	317.35	0.7	83.0	88.8	7.16	117	21.88
TM710	79,663	20,737	339.66	0.7	69.5	94.4	6.71	126	24.05
BW30LE	77,478	22,522	367.79	0.7	79.8	102.1	6.92	137.51	26.12

Table 7
Cost evaluation cost of the produced cubic meter for the three membranes

	NF90	TM710	BW30LE
Number of modules	262	480	367
Capital cost (€)	422,697.134	609,374.475	512,384.939
Annual operating cost (€/y)	9,106.840681	13,128.7293	11,039.12857
Annual membrane replacement costs (€/y)	5,247.930142	9,596.004843	7,336.931818
Energy cost (€/m ³)	0.036	0.036	0.036
Total cost (€/m ³)	0.1228	0.1640	0.1426

(NF90). The comparison of the performances of those membranes is carried out for removing fluoride ions.

In continuous mode, the behavior of NF90*4040 membrane in reducing fluoride and all others ions content is similar to that of BW30LE4040 and TM710 RO membranes, due to the structure of the NF90 membrane which is close to that of RO membranes ones. The permeate flux follows the following order: NF90 > BW30LE4040 > TM710.

The application of the Spiegler–Kedem model to determine the constants of the model namely the reflection coefficient and the coefficient of permeability shows a good agreement between experimental model release rates and transport mechanism in these membranes, which is of purely diffusive nature.

In semi-batch mode, the permeate flux decreases with the increase of recovery rate but the ions content increases slightly in the permeate. Precipitation occurs in the retentate at recovery rate of 84% for NF90 and 80% for both TM710 and BW30LE.

The use of Hermia model allows identifying the fouling mechanism that occurs during NF and RO processes. Calculation parameters of Hermia model show that the mechanism, which describes experimental data for the three studied membranes is the cake forming model.

The economic evaluation shows that the cost of the produced cubic meter by the three membranes is almost the same but defluoridation with NF membrane remains slightly less expensive in comparison with the two other membranes. The cost follows the following order: NF90 < BW30LE4040 < TM710.

Acknowledgments

This work was supported by ONEE Co., (Morocco) and TIA Co., (France). The authors express their thanks for this support.

References

- [1] M. Bodzek, K. Konieczny, Removal of fluoride from aquatic environment, *J. Desal. Water Treat.*, 117 (2018) 118–141.
- [2] S.V. Jadhav, E. Bringas, G.D. Yadav, V.K. Rathod, I. Ortiz, K.V. Marathe, Arsenic and fluoride contaminated groundwaters: a review of current technologies for contaminants removal, *J. Environ. Manage.*, 162 (2015) 306–325.
- [3] J. Shen, A. Schafer, Removal of fluoride and uranium by nanofiltration and reverse osmosis: a review, *Chemosphere*, 117 (2014) 679–691.
- [4] J. Fawell, K. Bailey, J. Chilton, E. Dahi, L. Fewtrell, Y. Magara, Fluoride in Drinking Water, World Health Organization, London, 2006.
- [5] A.B. Koltuniewicz, E. Drioli, Membranes in Clean Technologies, Wiley-VCH Verlag GmbH, Weinheim, 2008.
- [6] N. Mameri, A.R. Yeddou, H. Lounici, H. Grib, D. Belhocine, B. Bariou, Defluoridation of septentrional Sahara water of North Africa by electrocoagulation process using bipolar aluminium electrodes, *Water Res.*, 32 (1998) 1604–1610.
- [7] M. Tahaikt, A. Ait Haddou, R. El Habbani, Z. Amor, F. Elhannouni, M. Taky, M. Khariif, A. Boughriba, M. Hafsi, A. Elmidaoui, Comparison of the performances of three commercial membranes in fluoride removal by nanofiltration. Continuous operations, *Desalination*, 225 (2008) 209–219.
- [8] M. Tahaikt, R. El Habbani, A. Ait Haddou, I. Achary, Z. Amor, M. Taky, A. Alami, A. Boughriba, M. Hafsi, A. Elmidaoui, Fluoride removal from groundwater by nanofiltration, *Desalination*, 212 (2007) 46–53.
- [9] Meenakshi, R.C. Maheshwari, Fluoride in drinking water and its removal, *J. Hazard. Mater.*, 137 (2006) 456–463.
- [10] S.S. Waghmare, T. Arfin, Fluoride removal from water by various techniques: review, *Int. J. Innovative Sci. Eng. Technol.*, 2 (2015) 560–571.
- [11] G. Singh, B. Kumar, P.K. Sen, J. Majumdar, Removal of fluoride from spent pot liner leachate using ion exchange, *Water Environ. Res.*, 71 (1999) 36–42.
- [12] B. Solangi, S. Memon, M.I. Bhangar, An excellent fluoride sorption behavior of modified amberlite resin, *J. Hazard. Mater.*, 176 (2010) 186–192.
- [13] S.P. Kamble, P. Dixit, S.S. Rayalu, N.K. Labhsetwar, Defluoridation of drinking water using chemically modified bentonite clay, *Desalination*, 249 (2009) 687–693.
- [14] M.A. Menkouchi Sahli, S. Annouarb, M. Tahaikt, M. Mountadar, A. Soufiane, A. Elmidaoui, Fluoride removal for underground brackish water by adsorption on the natural chitosan and by electro dialysis, *Desalination*, 212 (2007) 37–45.
- [15] M. Tahaikt, I. Achary, M.A. Menkouchi Sahli, Z. Amor, M. Taky, A. Alami, A. Boughriba, M. Hafsi, A. Elmidaoui, Defluoridation of Moroccan groundwater by electro dialysis: continuous operation, *Desalination*, 189 (2006) 215–220.
- [16] C.K. Diawara, S.N. Diop, M.A. Diallo, M.A. Farcy, Determination performance of nanofiltration (NF) and low pressure reverse osmosis (LPRM) membranes in the removal of fluorine and salinity from brackish drinking water, *Water Resour. Prot.*, 3 (2011) 912–917.
- [17] V.V. Gedam, J.L. Patil, S. Kagne, R.S. Sirsam, P. Labhsetwar, Performance evaluation of polyamide reverse osmosis membrane for removal of contaminants in ground water collected from Chandrapur district, *J. Membr. Sci. Technol.*, 2 (2012) 1–5.
- [18] J.J. Schoeman, Water Defluoridation, Water Denitrification and Water Desalination in Rural Areas in South Africa, Proceedings of Third IASTED African Conference, Power and Energy System (AfricaPES 2010), Gaborone, Botswana, 2010, pp. 244–247.
- [19] V.B. Briao, J. Magoga, M. Hemkemeier, E.B. Briao, L. Girardelli, L. Sbeghen, D.P.C. Favaretto, Reverse osmosis for desalination of water from the Guarani aquifer system to produce drinking water in southern Brazil, *Desalination*, 344 (2014) 402–411.
- [20] F. Elazhar, M. Tahaikt, A. Achatei, F. Elmidaoui, M. Taky, F. El Hannouni, I. Laaziz, M. El Amrani, A. Elmidaoui, S. Jariri, Economical evaluation of the fluoride removal by nanofiltration, *Desalination*, 249 (2009) 154–157.
- [21] A.H. Bannoud, Y. Darwich, Elimination des ions fluorure et manganèse contenus dans les eaux par nanofiltration, *Desalination*, 206 (2007) 449–456.
- [22] M. Pontié, H. Buisson, C.K. Diawara, H. Essis-Tome, Studies of halide ions mass transfer in nanofiltration-application to selective defluorination of brackish drinking water, *Desalination*, 157 (2003) 127–134.
- [23] A.W. Mohammad, Y.H. Teow, W.L. Ang, Y.T. Chung, D.L. Oatley-Radcliffe, N. Hilal, Nanofiltration membrane review: recent advances and future prospects, *Desalination*, 356 (2015) 226–254.
- [24] N. Zouhri, M. Igouzal, M. Larif, M. Hafsi, M. Taky, A. Elmidaoui, Prediction of salt rejection by nanofiltration and reverse osmosis membranes using Spiegler-Kedem model and an optimisation procedure, *Desal. Water Treat.*, 120 (2018) 41–50.
- [25] R.R. Nair, E. Protasova, S. Strand, T. Bilstad, Implementation of Spiegler–Kedem and steric hindrance pore models for analyzing nanofiltration membrane performance for smart water production, *Membranes (Basel)*, 8 (2018), doi: 10.3390/membranes8030078.
- [26] A. Fatehizadeha, M.M. Amin, M. Sillanpää, N. Hatami, E. Taheri, N. Baghaei, S. Mahajan, Modeling of fluoride rejection from aqueous solution by nanofiltration process: single and binary solution, *Desal. Water Treat.*, 193 (2020) 224–234.
- [27] I. Bejaoui, A. Mnif, B. Hamrouni, Influence of operating conditions on the retention of fluoride from water by nanofiltration, *Desal. Water Treat.*, 29 (2011) 39–46.

- [28] A. Charfi, N. Ben Amar, J. Harmand, Analysis of fouling mechanisms in anaerobic membrane bioreactors, *Water Res.*, 46 (2012) 2637–2650.
- [29] F. Elazhar, J. Tourir, M. Elazhar, S. Belhamidi, N. El Harrak, A. Zdeg, M. Hafsi, Z. Amor, M. Taky, A. Elmidaoui, Techno-economic comparison of reverse osmosis and nanofiltration in desalination of a Moroccan brackish groundwater, *Desalination and Water Treatment*, (2014) 1–7.
- [30] W. Guo, H.H. Ngo, J. Li, A mini-review on membrane fouling, *Bioresour. Technol.*, 122 (2012) 27–34.
- [31] S. Lahmid, M. Tahaikt, K. Elaroui, I. Idrissi, M. Hafsi, I. Laaziz, Z. Amor, F. Tiyal, A. Elmidaoui, Economic evaluation of fluoride removal by electrodialysis, *Desalination*, 230 (2008) 213–219.
- [32] S. El-Ghizel, H. Zeggar, M. Tahaikt, F. Tiyal, A. Elmidaoui, M. Taky, Nanofiltration process combined with electrochemical disinfection for drinking water production: feasibility study and optimization, *J. Water Process Eng.*, 36 (2020), doi: 10.1016/j.jwpe.2020.101225.
- [33] RAYMOND, Desjardins, *Le Traitement Des Eaux*, Presses Internationales POLYTECHNIQUE, 2nd éd., Canada, 1997.
- [34] *Guidelines for Drinking-Water Quality: Fourth Edition Incorporating the First Addendum* ISBN 978-92-4-154995-0.
- [35] Moroccan Official Bulletin. Joint Orders No. 1275-01, 1276-01 and 1277-01 of 17th October 2002 Defining the Quality Norms of Surface Waters, Waters Destined for Irrigation and of Surface Waters Used for the Production of Drinking Water Respectively; Official Bulletin of the Kingdom of Morocco no. 5062; Moroccan Official Bulletin: Rabat, Morocco, 2002; pp. 1518–1525.